Journal of The Electrochemical Society, **156** (7) H505-H511 (2009)
0013-4651/2009/156(7)/H505/7/$25.00 © The Electrochemical Society

Removal of Ion-Implanted Photoresists Using Wet Ozone

Masashi Yamamoto,[a,z] Yousuke Goto,[a] Takeshi Maruoka,[a] Hideo Horibe,[a,c] Toshinori Miura,[b] Eiji Kusano,[a] and Seiichi Tagawa[c]

[a]*Kanazawa Institute of Technology, Ishikawa 924-0838, Japan*
[b]*Central Research Laboratory, Meidensha Corporation, Shizuoka 410-8588, Japan*
[c]*The Institute of Scientific and Industrial Research, Osaka University, Osaka 567-0047, Japan*

Using environmentally friendly wet ozone instead of chemicals, we removed B-, P-, and As-ion-implanted positive-tone novolak photoresists with an implantation dose of 5×10^{12}–1×10^{16} atoms/cm^2 at an acceleration energy of 70 keV. Ion-implanted photoresists with an implantation dose exceeding 5×10^{15} atoms/cm^2 could not be removed, but photoresists implanted at doses below 5×10^{13} atoms/cm^2 could be removed. Photoresist implanted with B ions at 5×10^{14} atoms/cm^2 was removed slowly, but photoresists implanted with P and As ions were not removed at all. The hardness of the photoresist with B ions implanted at 5×10^{14} atoms/cm^2 was 1.8 times greater than that of the nonimplanted photoresist (AZ6112), that of the P-ion-implanted photoresist was eight times greater, and that of the As-ion-implanted photoresist was five times greater. The B-ion-implanted photoresist was softer than the P- and As-ion-implanted photoresists. We also obtained the calculation results in which the energy supplied from the B ions to the photoresist was lower than that from P and As ions. We assumed that the ion-implanted photoresists were hardened by cross-linkage due to the energies supplied to the photoresists from the ions. Therefore, we determined that the hardness threshold of the photoresist that could be removed by using wet ozone was twice the hardness of AZ6112.
 [DOI: 10.1149/1.3121583]

Manuscript submitted January 20, 2009; revised manuscript received March 10, 2009. Published April 27, 2009.

In the semiconductor manufacturing process, semiconductor devices are formed on Si-wafer substrates using several processes (e.g., coating, photoresist patterning, etching, ion implantation, photoresist removal, and cleaning). Ion implantation is one of the most important processes in fabricating p/n semiconductor devices. In the ion-implantation process, group 13 or 15 elements (e.g., B, P, and As ions) are irradiated over the entire area of the substrate on which photoresist patterns have been fabricated. The ions are implanted into the photoresist, which can also play a role as a mask for the substrate. It is difficult to remove the ion-implanted photoresist because the photoresist hardens and gets denatured by implanted ions. The ion-implanted photoresist is actually removed by combining oxygen plasma ashing and chemicals such as sulfuric acid–hydrogen peroxide mixture (SPM) or ammonia–hydrogen peroxide mixture (APM), although the removal of the photoresist is troublesome at the present time. However, oxygen plasma ashing may cause unwanted oxidation of the substrates and metal interconnects. The problems associated with the photoresist removal process are described below. A cleaning process using ultrapure water is necessary to remove particles (e.g., residues) when 25 wafers are treated by SPM in a batch process because SPM may not remove all the particles. It is important to control mixture timing to remove ion-implanted photoresist because SPM has the highest reactivity just when sulfuric acid and hydrogen peroxide are mixed. Therefore, those chemicals must be kept fresh, and it is very expensive to separate and purify mixture chemicals. APM has some problems (e.g., short lifetime, deposition of metal impurities, and increase in surface microroughness). A very thin SiO_2 isolation layer may be etched by APM in advanced nanotechnology (e.g., 45 nm technology) because APM can etch into Si and SiO_2 at a rate of a few Å/min.[1,2]

In this study, we investigated the relationship between ion-implanted photoresist removal using environmentally friendly wet ozone and hardness of the photoresist by ion implantation. In the wet-ozone process developed at Mitsubishi Electric Corp., the photoresist is hydrolyzed to a water-soluble carboxylic acid by adding a trace amount of water during the reaction of ozone with the photoresist.[3-5] The wet-ozone process is a very environmentally friendly photoresist removal method compared to chemical methods because it contributes in reducing removal costs that are largely composed of chemical costs and residual ozone returns to oxygen. Wet ozone also has a cleaning effect on the substrates. Wet ozone using acetic acid instead of water can prevent the oxidation of metal by controlling the ionization of carboxylic acid.[6] Using wet ozone, we removed positive-tone novolak photoresists implanted with B, P, and As ions at an implantation dose of 5×10^{12}–1×10^{16} atoms/cm^2 at 70 keV of acceleration energy. In general, the ion-implanted photoresist subsurface layer through which the ions passed might be hardened.[7-11] The photoresist hardness, however, has not yet been quantitatively evaluated. Using nanoindentation[12-15] to measure the hardness of the ion-implanted photoresists, we demonstrated the relationship between removal performance and hardness of ion-implanted photoresists. We used SRIM2008 (stopping range of ions in materials)[16] to simulate the interaction of the implanted ions and the photoresists.

Experimental

Ion-implanted photoresist removal using wet ozone.— Figure 1 presents a schematic diagram of the wet-ozone experiment apparatus (Mitsubishi Electric Corp. and SPC Electronics Corp.). Ozone gas was generated by an ozonizer (OP-300C-S; Mitsubishi Electric Corp.) at a density of 230 g/m^3 (10.2 vol %) and a flow rate of 12.5 L/min. Wet ozone means ozone gas with vapor water. Wet ozone

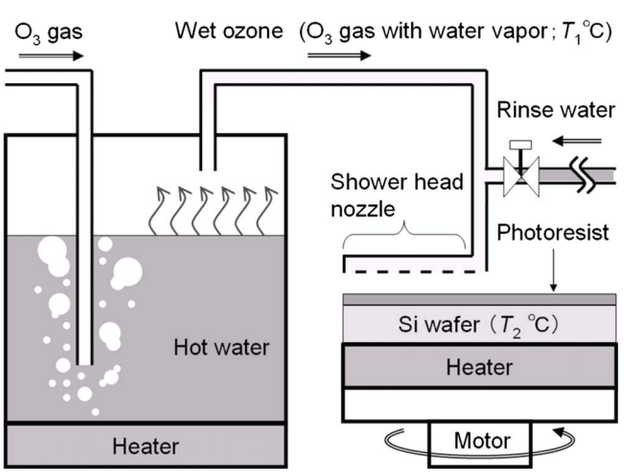

Figure 1. (Color online) Schematic diagram of the experiment apparatus.

[z] E-mail: m-yamamoto@venus.kanazawa-it.ac.jp

Table I. Experiment conditions for photoresist removal by wet ozone.

Parameter	Value
Wet-ozone temperature (T_1)	60°C
Substrate temperature (T_2)	50°C
Wet-ozone irradiation time ($t_{wet\text{-}o3}$) per cycle	10 s
Rinse water temperature	70°C
Rinse time per cycle	5 s
Drying time per cycle	10 s
Wet-ozone process time (t_{proc}) per cycle	25 s
Substrate rotation rate	2000 rpm
Ozone gas density	230 g/m^3 (10.2 vol %)
Ozone gas flow rate	12.5 L/min

generated by bubbling ozone gas through hot water was irradiated onto the photoresists from a showerhead nozzle. The wet ozone could be uniformly irradiated onto the entire surface of the photoresists by rotating the substrates at 2000 rpm. A trace amount of water to hydrolyze the photoresists to carboxylic acid was finely adjusted by controlling the amount of dew condensation water according to the difference between the temperature of the wet ozone (T_1 = 60°C) and that of the substrate (T_2 = 50°C). Table I lists the experiment conditions for the photoresist removal. In the wet-ozone process, the photoresist was gradually decomposed and removed from the surface. Specifically, the photoresist surface layer was hydrolyzed to carboxylic acid, which was washed off with pure water. For that reason, three treatments (wet-ozone irradiation, pure-water washing, and drying) were repeated in a cycle of the removal, using wet ozone. The treatment cycle consisted of 10 s of wet-ozone irradiation, 5 s of pure-water washing, and 10 s of drying. The wet-ozone processing time (t_{proc}) was the summation of all treatment times and cycles. In this experiment, we evaluated the relationship between ion-implanted photoresist removal and wet-ozone irradiation time ($t_{wet\text{-}o3}$) by measuring the photoresist film thickness every few cycles. The wet-ozone processing time takes two and a half times longer than the wet-ozone irradiation time.

A positive-tone novolak photoresist (AZ6112; AZ-Electronic Materials) was used for this study. It was spin-coated onto a Si wafer using a spin coater (ACT-300A; Active) at 2000 rpm for 20 s and then prebaked at 100°C for 1 min on a hotplate (PMC 720 series; Dataplate). The photoresist film thickness (0.9–1.0 μm) was measured using a stylus-type surface profile measurement instrument (DekTak 6M; ULVAC). The B, P, and As ions were implanted into the photoresists at a dose of 5×10^{12}–1×10^{16} atoms/cm^2 and an acceleration energy of 70 keV without wafer cooling. During implantation, the pressure inside the chamber was 10^{-6} Pa. The initial substrate temperature was 23°C (room temperature); however, the temperature was not monitored during implantation. Table II lists the film thickness, ion current, and implantation time for the ion-implanted photoresist. We investigated the relationship between the removal performance using wet ozone and the hardening of the ion-implanted photoresist.

Measurement of ion-implanted photoresist using nanoindentation.— Figure 2 presents a schematic diagram of the evaluation of the hardness of the ion-implanted photoresist using nanoindentation (ENT-1040; ELIONIX). In nanoindentation, we obtained a loading–unloading curve (Fig. 2 I-II) that consisted of a loading curve, a load holding, and an unloading curve. Here, P and h_1 were the maximum load and the indentation depth (point p). Table III lists the experiment conditions for nanoindentation. We examined the hardnesses at various depths (h_1) by changing the maximum loads from 1 to 360 mgf. The loading–unloading rate was set at 0.004 mgf/ms (lower limit) for a load of 1–8 mgf and at 1/2000 of load for a load of more than 8 mgf. The load-holding time between loading and unloading was 2 s. We evaluated the plastic-deformation hardness obtained from the unloading curves at various loads for the ion-implanted photoresists using a Berkovich-type diamond indenter with an apex angle of 115°. In nanoindentation, the plastic-deformation hardness at h_1 was obtained from plastic-deformation depth (h_2), which is

Table II. Film thickness, ion current, and implantation time for the ion-implanted photoresist.

Ion species (at 70 keV)	Implantation dose (atoms/cm^2)	Film thickness (μm)	Ion current (μA)	Implantation time (s)
—	Nonimplantation	0.9–1.0	—	—
B	5×10^{12}	0.84	4.5	33
B	5×10^{13}	0.85	29.3	51
B	5×10^{14}	0.85	46.9	320
B	5×10^{15}	0.73	61.6	2410
B	1×10^{16}	0.68	60.0	4940
P	5×10^{12}	0.99	4.9	38
P	5×10^{13}	0.99	31.0	48
P	5×10^{14}	0.95	52.8	282
P	5×10^{15}	0.93	63.5	2325
P	1×10^{16}	0.86	59.5	5038
As	5×10^{12}	0.98	5.0	30
As	5×10^{13}	0.93	30.9	49
As	5×10^{14}	0.86	53.6	278
As	5×10^{15}	0.78	61.5	2435
As	1×10^{16}	0.75	60.1	4944

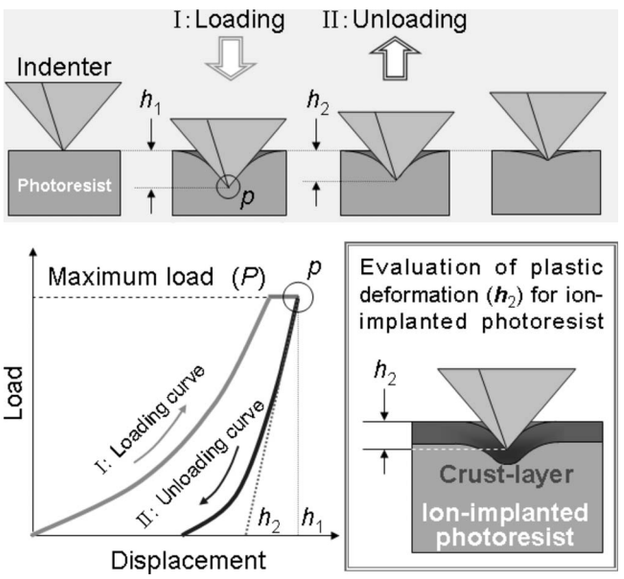

Figure 2. Schematic diagram of the nanoindentation experiment apparatus. Here, h_1 and h_2 are indentation depth and plastic-deformation depth.

Table III. Experiment conditions for evaluating ion-implanted photoresist hardness by nanoindentation.

Parameter	Value
Maximum load	320 mgf
Loading–unloading rate (1–8 mgf)	0.004 mgf/ms
Loading–unloading rate (more than 8 mgf)	(Load/2000) mgf/ms
Load-holding time	2 s
Indenter material	Diamond
Indenter type	Berkovich (apex angle of 115°)

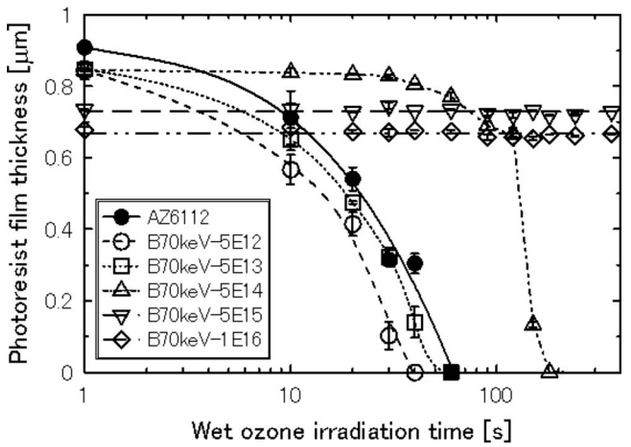

Figure 3. Dependence of B-ion-implanted photoresist film thickness on wet-ozone irradiation time (log). AZ6112 was a positive-tone novolak photoresist without ion implantation. B-ion-implantation doses were 5×10^{12}–1×10^{16} atoms/cm^2, and the B-ion-acceleration energy was 70 keV.

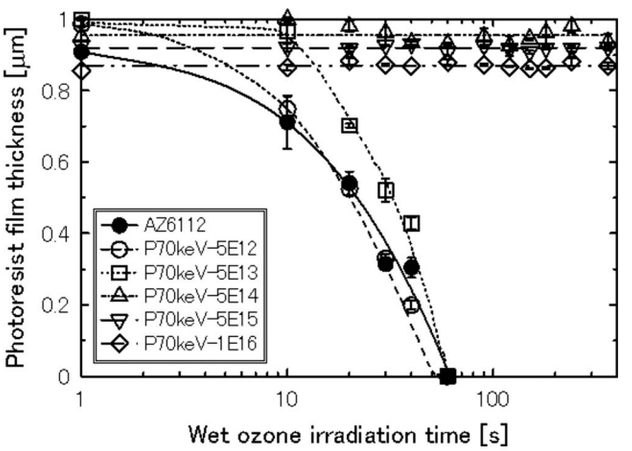

Figure 4. Dependence of the P-ion-implanted photoresist film thickness on wet-ozone irradiation time (log). AZ6112 was a positive-tone novolak photoresist without ion implantation. P-ion-implantation doses were 5×10^{12}–1×10^{16} atoms/cm^2, and the P-ion-acceleration energy was 70 keV.

tangent to the unloading curve from p intersected on the x axis and indicated the plasticity of the sample at h_1. The plastic deformation hardness was defined as

$$H_2 = K\frac{P\ (\text{mgf})}{h_2^2\ (\mu\text{m}^2)} \qquad [1]$$

where K is a factor attributable to the indenter configuration and was 37.926 with the use of a Berkovich-type indenter. We measured plastic-deformation hardness at various indentation depths to determine the depth profiles of the hardness of the ion-implanted photoresists. We evaluated the hardness of the ion-implanted photoresist normalized by the hardness of the nonimplanted photoresist (H_2 of AZ6112); we defined that normalized H_2. Normalized H_2 was obtained by dividing H_2 of the ion-implanted photoresist by H_2 of AZ6112.

Investigation of energies supplied from ion to photoresist about hardening of the ion-implanted photoresist.— We examined the ion-implanted photoresists by numeric simulations. It is generally difficult to remove ion-implanted photoresists because they may harden due to thermal cross-linking or carbonization by energy supplied from implanted ions.[7-11] Using SRIM, we calculated the energies supplied from implanted ions to the photoresist (elements such as C, O, and H, which are components of the photoresist). We used polymethylmethacrylate (PMMA) as the photoresist because it was complicated for the SRIM to incorporate the effect of resonance stability of benzene rings in novolak photoresists into the calculations. The novolak photoresist includes a benzene ring being energetically stable, so its stopping power is probably higher than that of PMMA. Accordingly, implanted ions may be distributed toward the surface, and also the energies supplied to the photoresists from ions are perhaps larger than that supplied to PMMA. However, we can get relative tendencies of the energies and the distributions for each ion. Therefore, we relativized the energies supplied from the ions to the photoresist because we cannot discuss the absolute value from the calculation results.

Results and Discussion

Ion-implanted photoresist removal using wet ozone.— Figure 3 depicts the change in B-ion-implanted photoresist film thickness with respect to wet-ozone irradiation time (log) at various implantation doses. The film thickness of photoresists with a B-ion-implantation dose of 5×10^{12}–5×10^{13} atoms/cm^2, as well as that of AZ6112, decreased with an increase in wet-ozone irradiation time. The removal rate of the photoresist with a dose of 5×10^{12} atoms/cm^2 was 1.26 μm/min ($t_{\text{wet-o3}} = 40$ s) and that with a dose of 5×10^{13} atoms/cm^2 was 0.83 μm/min ($t_{\text{wet-o3}} = 60$ s). The removal rate of the photoresist with 5×10^{13} atoms/cm^2 slightly decreased compared to that with 5×10^{12} atoms/cm^2. For the photoresist with a dose of 5×10^{14} atoms/cm^2, the decrease in film thickness was hardly observed until 120 s of wet-ozone irradiation time; however, it was possible to remove that photoresist as well as AZ6112 after 120 s. Eventually, the photoresist with a dose of 5×10^{14} atoms/cm^2 was removed at a rate of 0.28 μm/min ($t_{\text{wet-o3}} = 180$ s). Although the above removal rates were calculated from the ozone irradiation time, the removal rates obtained from the total processing time were 0.50 μm/min ($t_{\text{proc}} = 100$ s, 4 cycles), 0.40 μm/min ($t_{\text{proc}} = 125$ s, 5 cycles), and 0.11 μm/min ($t_{\text{proc}} = 450$ s, 18 cycles), respectively. The film thickness of photoresists with doses exceeding 5×10^{15} atoms/cm^2 remained unchanged with increased wet-ozone irradiation time. It was thus impossible to remove the photoresist using wet ozone. The removal rate decreased with increasing implantation dose; it was more difficult to remove the photoresist with the higher dose.

Figure 4 depicts the change in P-ion-implanted photoresist film thickness with wet-ozone irradiation time (log) at various implantation doses. The film thickness of the photoresists with a P-ion-implantation dose of 5×10^{12}–5×10^{13} atoms/cm^2, as well as that of the B-ion-implanted photoresists with the same implantation dose, decreased with increasing wet-ozone irradiation time. The photoresist removal rate with a dose of 5×10^{12} atoms/cm^2 was 1.19 μm/min ($t_{\text{wet-o3}} = 50$ s) and that with a dose of 5×10^{13} atoms/cm^2 was 0.99 μm/min ($t_{\text{wet-o3}} = 60$ s). The removal rates obtained from the total processing time were 0.48 μm/min ($t_{\text{proc}} = 125$ s, 5 cycles) and 0.40 μm/min ($t_{\text{proc}} = 150$ s, 6 cycles), respectively. The removal rate with a dose of 5×10^{13} atoms/cm^2 also slightly decreased compared to that with 5×10^{12} atoms/cm^2, like the B-ion-implanted photoresists. However, it was impossible to remove the P-ion-implanted photoresist with a dose of 5×10^{14} atoms/cm^2, unlike the B-ion-implanted photoresist that was slowly removed. It was also impossible to remove the photoresists with a dose exceeding 5×10^{15} atoms/cm^2, as well as the B-ion-implanted photoresists, by using wet ozone.

Figure 5 depicts the change in As-ion-implanted photoresist film thickness with wet-ozone irradiation time (log) at various implantation doses. The photoresist removal rate with an implantation dose of 5×10^{12} atoms/cm^2 was 1.28 μm/min ($t_{\text{wet-o3}} = 46$ s) and that with a dose of 5×10^{13} atoms/cm^2 was 0.90 μm/min ($t_{\text{wet-o3}} = 62$ s). The removal rates obtained from the total processing time

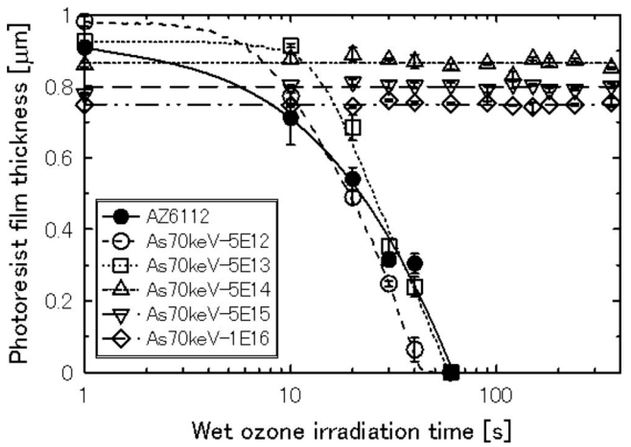

Figure 5. Dependence of the As-ion-implanted photoresist film thickness on wet-ozone irradiation time (log). AZ6112 was a positive-tone novolak photoresist without ion implantation. As-ion-implantation doses were 5×10^{12}–1×10^{16} atoms/cm^2, and the As-ion-acceleration energy was 70 keV.

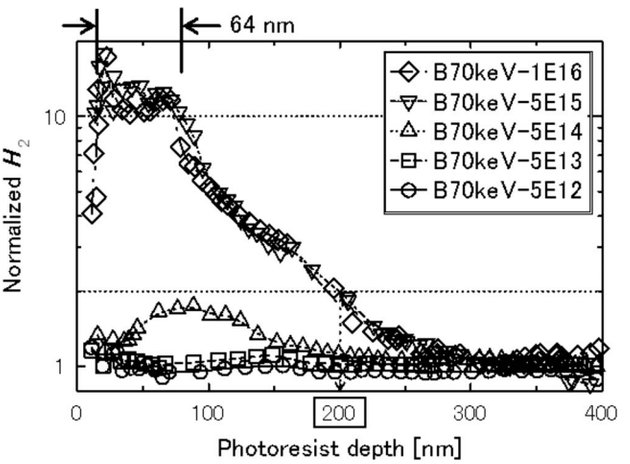

Figure 6. Depth profiles of normalized plastic-deformation hardness (normalized H_2) of the B-ion-implanted photoresists. Normalized H_2 was obtained by dividing H_2 of ion-implanted photoresist by H_2 of AZ6112. The B-ion-implantation doses were 5×10^{12}–1×10^{16} atoms/cm^2, and the B-ion-acceleration energy was 70 keV.

were 0.47 μm/min (t_{proc} = 125 s, 5 cycles) and 0.35 μm/min (t_{proc} = 150 s, 6 cycles), respectively. It was impossible to remove the photoresists with doses exceeding 5×10^{14} atoms/cm^2, as well as the P-ion-implanted photoresists, by using wet ozone.

Consequently, it was possible to remove ion-implanted photoresists with implantation doses below 5×10^{13} atoms/cm^2 by using wet ozone. The removal rate with 5×10^{13} atoms/cm^2 slightly decreased compared to that with 5×10^{12} atoms/cm^2. For doses of 5×10^{14} atoms/cm^2, only the B-ion-implanted photoresist was removed, although removal was slow. It was impossible to remove the ion-implanted photoresist with doses exceeding 5×10^{15} atoms/cm^2 by using wet ozone. These results indicated that a surface-hardened layer might form at the surface of the photoresist when doses exceed 5×10^{14} atoms/cm^2. However, the fact that only the B-ion-implanted photoresist with 5×10^{14} atoms/cm^2 was removed implies that the surface-hardened layer of the B-ion-implanted photoresist was softer than that of the P- and As-ion-implanted photoresists at the same dose. We therefore examined the hardness of the ion-implanted photoresists to consider differences in removal performance due to ion species and implantation doses.

Hardness of the ion-implanted photoresist.— Figure 6 depicts the depth profiles of the normalized plastic-deformation hardness of the B-ion-implanted photoresists measured by nanoindentation. Normalized H_2 was obtained by dividing H_2 of ion-implanted photoresist by H_2 of AZ6112, a photoresist without ion implantation. The photoresists with doses below 5×10^{13} atoms/cm^2 had almost the same hardness as AZ6112. The hardness of photoresists with doses exceeding 5×10^{14} atoms/cm^2 increased with increasing ion-implantation dose. A surface-hardened layer of the photoresist with a dose of 5×10^{14} atoms/cm^2 was formed at depths of 40–140 nm, and its peak was observed at a depth of 90 nm. However, the photoresists with doses exceeding 5×10^{15} atoms/cm^2 were generally hardened; for example, a surface-hardened layer with a hardness of more than 2 (normalized $H_2 \geq 2$) was observed from the surface to 200 nm, and the width of the surface-hardened layer with a hardness of more than 10 (normalized $H_2 \geq 10$) was 64 nm. The peak of hardness of a photoresist with a dose of 5×10^{14} atoms/cm^2 was 1.8, and the peak hardness for a photoresist with a dose exceeding 5×10^{15} atoms/cm^2 was 19. In the B-ion-implanted photoresists, the peak of hardness was enhanced 10.6 times when the dose increased from 5×10^{14} to 5×10^{15} atoms/cm^2.

Figure 7 depicts the depth profiles of the normalized plastic-deformation hardness of the P-ion-implanted photoresists measured by nanoindentation. The photoresists with doses below 5×10^{13} atoms/cm^2 had almost the same hardness as AZ6112, as did the B-ion-implanted photoresists. The hardness of the photoresists with doses exceeding 5×10^{14} atoms/cm^2 also increased with increased ion-implantation dose. In the photoresists with doses of 5×10^{14} atoms/cm^2, a normalized $H_2 \geq 2$ was observed from the surface to 75 nm depth. In the photoresists with doses exceeding 5×10^{15} atoms/cm^2, the normalized $H_2 \geq 2$ was observed from the surface to 155 nm depth, and the width of the normalized $H_2 \geq 10$ was 43 nm. The surface-hardened layer of the P-ion-implanted photoresists with doses exceeding 5×10^{14} atoms/cm^2 shifted toward the surface of the photoresists, compared with the B-ion-implanted photoresists with the same implantation dose. The peak of hardness for the photoresist with a dose of 5×10^{14} atoms/cm^2 was 6.3 and that for the photoresist with a dose exceeding 5×10^{15} atoms/cm^2 was 17. In the P-ion-implanted photoresists, the peak of hardness was enhanced by 2.1 times when the dose increased from 5×10^{14} to 5×10^{15} atoms/cm^2.

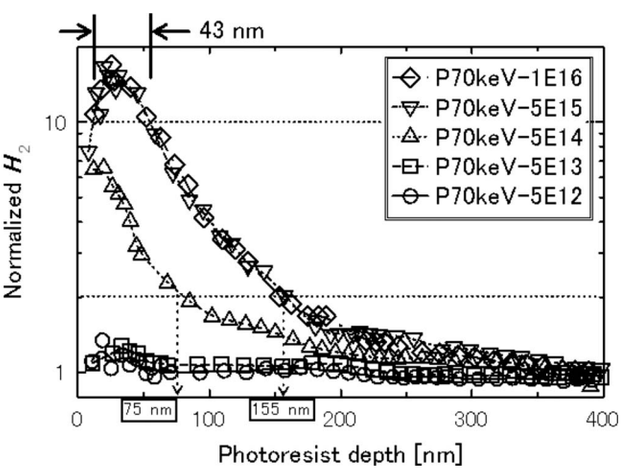

Figure 7. Depth profiles of normalized plastic-deformation hardness (normalized H_2) of the P-ion-implanted photoresists. Normalized H_2 was obtained by dividing H_2 of the ion-implanted photoresist by H_2 of AZ6112. The P-ion-implantation doses were 5×10^{12}–1×10^{16} atoms/cm^2, and the P-ion-acceleration energy was 70 keV.

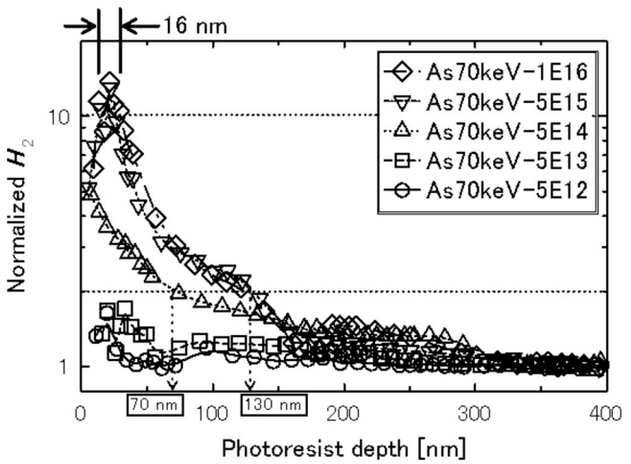

Figure 8. Depth profiles of normalized plastic-deformation hardness (normalized H_2) of As-ion-implanted photoresists. Normalized H_2 was obtained by dividing H_2 of ion-implanted photoresists by H_2 of AZ6112. The As-ion-implantation doses were 5×10^{12}–1×10^{16} atoms/cm^2, and the As-ion-acceleration energy was 70 keV.

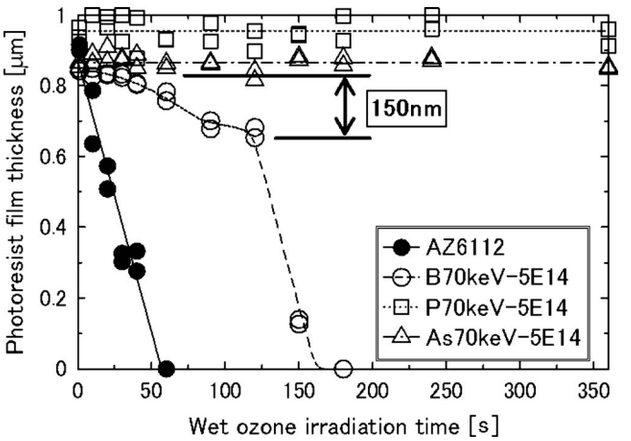

Figure 9. Dependence of the B-, P-, and As-ion-implanted photoresist film thicknesses on wet-ozone irradiation time. AZ6112 was a positive-tone novolak photoresist without ion implantation. The ion-implantation dose was 5×10^{14} atoms/cm^2, and the ion-acceleration energy was 70 keV.

Figure 8 depicts the depth profiles of normalized plastic-deformation hardness of the As-ion-implanted photoresists measured by nanoindentation. The photoresists with doses below 5×10^{13} atoms/cm^2 had almost the same hardness as AZ6112, as did the B- and P-ion-implanted photoresists. The hardness of photoresists with doses exceeding 5×10^{14} atoms/cm^2 also increased with increasing ion-implantation dose. In the photoresist with a dose of 5×10^{14} atoms/cm^2, the normalized $H_2 \geq 2$ was observed from the surface to a depth of 70 nm. In photoresists with doses exceeding 5×10^{15} atoms/cm^2, the normalized $H_2 \geq 2$ was observed from the surface to 130 nm depth, and the width of the normalized $H_2 \geq 10$ was 16 nm. The surface-hardened layer of As-ion-implanted photoresists with doses exceeding 5×10^{14} atoms/cm^2 shifted toward the surface of the photoresists compared with P-ion-implanted photoresists with the same implantation doses. The peak hardness for the photoresist with a dose of 5×10^{14} atoms/cm^2 was 5 and that for doses exceeding 5×10^{15} atoms/cm^2 was 13. In As-ion-implanted photoresists, the peak of hardness was enhanced 2.6 times when the dose increased from 5×10^{14} to 5×10^{15} atoms/cm^2.

The hardness of the photoresists with doses exceeding 5×10^{14} atoms/cm^2 increased with increasing ion-implantation dose (Fig. 6-8). However, we did not observe a difference in hardness according to implantation dose in photoresists with doses exceeding 5×10^{15} atoms/cm^2, possibly because the photoresist hardening due to ion implantation was likely saturated. Furthermore, the surface-hardened layer of photoresists with doses exceeding 5×10^{14} atoms/cm^2 shifted toward the surface of the photoresists with increasing atomic number of ions implanted into the photoresists. Table IV lists the surface-hardened layer (normalized $H_2 \geq 10$ and normalized $H_2 \geq 2$) of each ion-implanted photoresist obtained from the nanoindentation results of Fig. 6-8. The width of the surface-hardened layer decreased with increasing atomic number. Consequently, the hardening concentrated toward the surface of the photoresist with increasing atomic number. The energy supplied from implanted ions to the photoresist may have caused the formation of the surface-hardened layer and the hardening in the photoresist. Therefore, we investigated the relationship between the ion-implanted photoresist removal performance using wet ozone and the hardness of the photoresists with a dose of 5×10^{14} atoms/cm^2, which was perhaps the threshold for forming the surface-hardened layer.

Table IV. Surface-hardened layer (normalized $H_2 \geq 10$ and normalized $H_2 \geq 2$) for each ion-implanted photoresist obtained from the nanoindentation results of Fig. 6-8.

Ion-implantation dose (atoms/cm^2)	Hardness	B ions (nm)	P ions (nm)	As ions (nm)
5×10^{14}	Normalized $H_2 \geq 2$	—	75	70
5×10^{14}	Normalized $H_2 \geq 10$	—	—	—
5×10^{15} and 1×10^{16}	Normalized $H_2 \geq 2$	200	155	130
5×10^{15} and 1×10^{16}	Normalized $H_2 \geq 10$	64	43	16

Investigation of hardening mechanism for the ion-implanted photoresist.— Figure 9 depicts the change in B-, P-, and As-ion-implanted photoresist film thicknesses with wet-ozone irradiation time at an implantation dose of 5×10^{14} atoms/cm^2, as indicated in Fig. 3-5, respectively. The film thickness of AZ6112 decreased in direct proportion to wet-ozone irradiation time. The P- and As-ion-implanted photoresists were not removed at all, even for a wet-ozone irradiation of 360 min. In only the B-ion-implanted photoresist, the film thickness gradually decreased until the surface layer with 150 nm thickness was removed; then the film thickness decreased in direct proportion to wet-ozone irradiation time, like AZ6112. Figure 10 depicts the depth profiles of normalized plastic deformation hardness (normalized H_2) of the ion-implanted photoresists with a dose of 5×10^{14} atoms/cm^2, as indicated in Fig. 6-8. The surface-hardened layer of the B-ion-implanted photoresist was softer than that of P- and As-ion-implanted photoresists with that dose. The surface-hardened layer shifted toward the surface of the photoresists in order of increasing atomic numbers of ions implanted into the photoresists. The hardness of B-ion-implanted photoresist peaked at 90 nm depth with a ±50 nm width, and B-ion-implanted photoresist hardened 1.8 times more than AZ6112. The P-ion-implanted photoresist hardened up to eight times more than AZ6112, and the As-ion-implanted photoresist hardened up to five times more than AZ6112. Moreover, Fig. 11 depicts the relationship between the removal rates and the peak of hardness (normalized H_2) of the ion-implanted photoresists with doses below 5×10^{14} atoms/cm^2. When the normalized H_2 exceeded about 2, the photoresist removal rate could be 0 μm/min. Therefore, we determined that the hardness threshold of the photoresist that could be removed by using wet ozone was twice that of AZ6112. To consider differences in the surface-hardened layers among the ion species, we calculated the

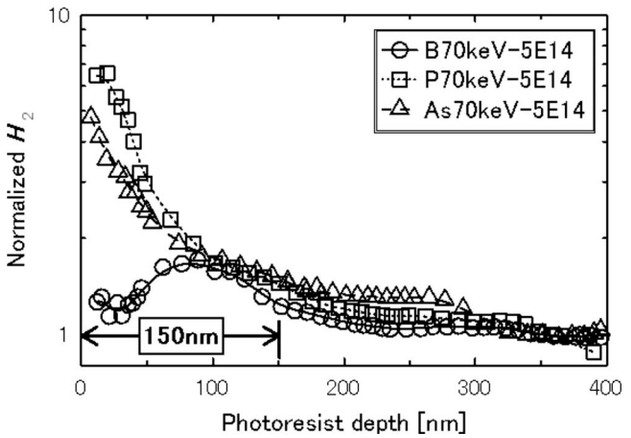

Figure 10. Depth profiles of normalized plastic-deformation hardness (normalized H_2) of the B-, P-, and As-ion-implanted photoresists with an ion-implantation dose of 5×10^{14} atoms/cm^2. Normalized H_2 was obtained by dividing H_2 of ion-implanted photoresist by H_2 of AZ6112. The ion-acceleration energy was 70 keV.

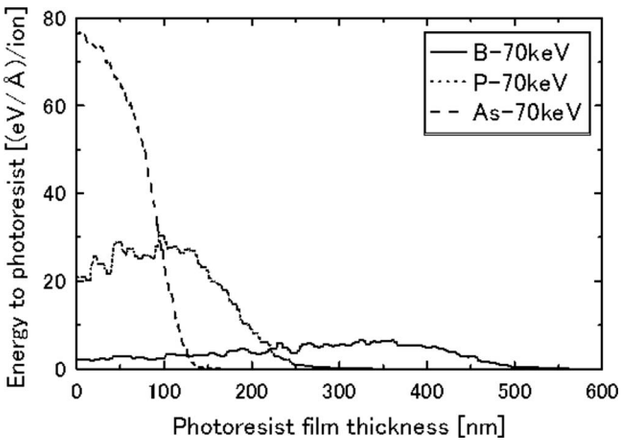

Figure 12. Distributions of the energies from B, P, and As ions to C, O, and H elements that compose PMMA were calculated by SRIM. The ion-acceleration energy was 70 keV.

distributions of the energies supplied from implanted ions to elements such as C, O, and H, which are components of the photoresists, using SRIM.

Figure 12 depicts the distributions of the energies supplied from each implanted ion to C, O, and H elements in the photoresist (PMMA). When the sum of energies supplied from the B ion to the photoresist was normalized to be 1, that from the P ion was 2.4 and that from the As ion was 3.4. It was found that the energies were more effectively supplied to the elements in the photoresist from the heavier ions. More energy was supplied to the photoresist and the distribution of the energy concentrated toward the surface with an increasing atomic mass. As indicated in Fig. 10, the surface-hardened layer shifted toward the surface and narrowed with increasing atomic mass. The distributions of energies were likely similar to the tendencies of the layer in ion-implanted photoresists. Therefore, we assumed that the energy concentration in the B-ion-implanted photoresist was lower than that in the P- and As-ion-implanted photoresists because B ions exchanged energies with the photoresist in wider regions than P and As ions (Fig. 11). Eventually, hardening of the ion-implanted photoresist might have been induced by cross-linking due to the energies supplied to the photoresist from the implanted ions[17] because a surface-hardened layer probably formed in the regions through which the ions passed. Accordingly, the surface of the photoresist hardened with increasing implantation dose (Fig. 6-8) because the energies increased with increasing dose. When we observed the ion-implanted photoresists with doses of 5×10^{14} atoms/cm^2 (Fig. 10), results indicated that the hardness of the surface-hardened layer in B-ion-implanted photoresist was lower than that of P- and As-ion-implanted photoresists. Consequently, only the B-ion-implanted photoresist with a dose of 5×10^{14} atoms/cm^2 was removed by using wet ozone because the B-ion-implanted photoresist hardened less than the P- and As-ion-implanted photoresists because the B ion exchanged less energies with the photoresist in wider regions than P and As ions.

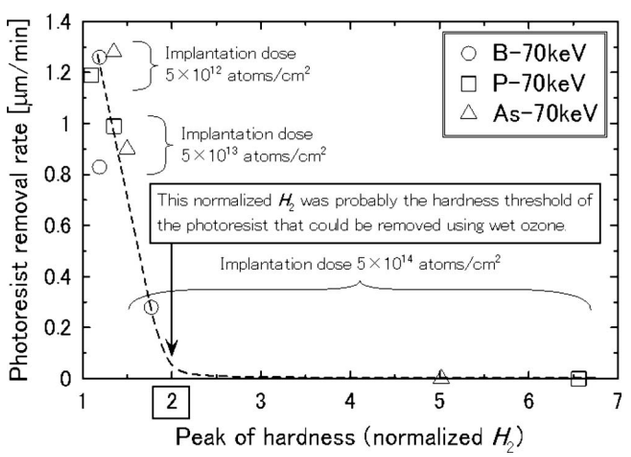

Figure 11. Relationship between the removal rates and the peak of hardness (normalized H_2) of the ion-implanted photoresists with doses below 5×10^{14} atoms/cm^2.

Conclusions

We clarified the relationship between ion-implanted photoresist removal using wet ozone and hardness of the photoresist induced by ion implantation. We also considered mechanisms of photoresist hardening using numerical simulation.

Using wet ozone, we removed positive-tone novolak photoresists into which B, P, and As ions were implanted at doses of 5×10^{12}–1×10^{16} atoms/cm^2 and an acceleration energy of 70 keV. The hardness of each ion-implanted photoresist with an implantation dose below 5×10^{13} atoms/cm^2 was similar to that of AZ6112, and it was possible to remove the ion-implanted photoresist similarly as for AZ6112. However, ion-implanted photoresists with doses exceeding 5×10^{15} atoms/cm^2 were more than 10 times harder than AZ6112, so they were impossible to remove. A B-ion-implanted photoresist with a dose of 5×10^{14} atoms/cm^2 was removed slowly, but P- and As-ion-implanted photoresists were not removed at all. The peak hardnesses of B-, P-, and As-ion-implanted photoresists with a dose of 5×10^{14} atoms/cm^2 reached 1.8 (B), 8 (P), and 5 (As) times more than AZ6112. The B-ion-implanted photoresist was softer than the P- and As-ion-implanted photoresists at that dose. Therefore, we determined that the hardness threshold of the photoresist that could be removed by using wet ozone was twice the hardness of AZ6112. The numerical simulation suggested that the energies were effectively supplied to the elements in the photoresist from the heavier implantation ion mass and that the distributions of the energies concentrated toward the surface with increasing atomic mass. These results suggested that only the B-ion-implanted photoresist with 5×10^{14} atoms/cm^2 could be removed by using wet ozone because it hardened less than the P- and As-ion-implanted photoresists because the B ions exchanged energies with the photoresist in wider regions than the P and As ions. We assumed that the

ion-implanted photoresists hardened by cross-linking due to the energies supplied to the photoresists from the implanted ions.

Acknowledgments

Part of this study was supported by an Industrial Technology Research Grant Program (2004) from the New Energy and Industrial Technology Development Organization (NEDO) of Japan, Mitsubishi Electric Corp., and SPC Electronics Corp.

Kanazawa Institute of Technology assisted in meeting the publication costs of this article.

References

1. M. Itano, F. W. Kern, Jr., M. Miyashita, and T. Ohmi, *IEEE Trans. Semicond. Manuf.*, **6**, 258 (1993).
2. K. Yamamoto, A. Nakamura, and U. Hase, *IEEE Trans. Semicond. Manuf.*, **12**, 288 (1999).
3. H. Horibe, M. Yamamoto, T. Ichikawa, T. Kamimura, and S. Tagawa, *J. Photopolym. Sci. Technol.*, **20**, 315 (2007).
4. S. Noda, M. Miyamoto, H. Horibe, I. Oya, M. Kuzumoto, and T. Kataoka, *J. Electrochem. Soc.*, **150**, G537 (2003).
5. S. Noda, H. Horibe, K. Kawase, M. Miyamoto, M. Kuzumoto, and T. Kataoka, *J. Adv. Oxid. Technol.*, **6**, 132 (2003).
6. S. Noda, K. Kawase, H. Horibe, I. Oya, M. Kuzumoto, and T. Kataoka, *J. Electrochem. Soc.*, **152**, G73 (2005).
7. S. Fujimura, J. Konno, K. Hikazutani, and H. Yano, *Jpn. J. Appl. Phys., Part 1*, **28**, 2130 (1989).
8. P. M. Visintin, M. B. Korzenshi, and T. H. Baum, *J. Electrochem. Soc.*, **153**, G591 (2006).
9. K. K. Ong, M. H. Liang, L. H. Chan, and C. P. Soo, *J. Vac. Sci. Technol. A*, **17**, 1479 (1999).
10. M. N. Kawaguchi, J. S. Papanu, and E. G. Pavel, *J. Vac. Sci. Technol. B*, **24**, 651 (2006).
11. M. N. Kawaguchi, J. S. Papanu, B. Su, M. Castle, and A. Al-Bayati, *J. Vac. Sci. Technol. B*, **24**, 657 (2006).
12. A. Nakaue and N. Kawakami, *Kobe Steel Engineering Reports*, **52**, 74 (2002).
13. M. Lichinchi, C. Lenardi, J. Haupt, and R. Vitali, *Thin Solid Films*, **312**, 240 (1998).
14. X. Chen and J. J. Vlassaka, *J. Mater. Res.*, **16**, 2974 (2001).
15. B. D. Beake, G. J. Leggett, and M. R. Alexander, *J. Mater. Sci.*, **37**, 4919 (2002).
16. J. F. Ziegler, J. P. Biersack, and U. Littmark, in *The Stopping and Range of Ions in Solids*, J. F. Ziegler, Editor, Pergamon, New York (1996).
17. T. C. Smith, in *Handbook of Ion Implantation Technology*, J. F. Ziegler, Editor, Elsevier Science, New York (1992).